MOLECULAR AND CELLULAR BIOLOGY, Jan. 1993, p. 659–667
0270-7306/93/010659-09$02.00/0

Vol. 13, No. 1

Differential Activation of *myc* Gene Family Members in Hepatic Carcinogenesis by Closely Related Hepatitis B Viruses

LORI J. HANSEN,[1] BUD C. TENNANT,[2] CHRISTOPH SEEGER,[3] AND DON GANEM[1]*

Howard Hughes Medical Institute and Department of Microbiology and Immunology, University of California, San Francisco, California 94143[1]; New York State College of Veterinary Medicine, Cornell University, Ithaca, New York 14853[2]; and Institute for Cancer Research, Philadelphia, Pennsylvania 19111[3]

Received 28 July 1992/Returned for modification 28 September 1992/Accepted 19 October 1992

Woodchucks infected with woodchuck hepatitis virus (WHV) and ground squirrels infected with ground squirrel hepatitis virus (GSHV) both develop hepatocellular carcinoma (HCC), but WHV-associated tumors arise more frequently and much earlier in life. These differences are preserved when the oncogenic potentials of the two viruses are examined in the same host (woodchucks). We examined RNA and genomic DNA from tumors arising from WHV- and GSHV-infected woodchucks to determine whether these viruses use the same oncogenic pathway. N-*myc* RNA was not expressed in normal liver but was expressed in 10 of 13 WHV-associated HCCs examined. Southern blot analysis showed that 7 of 17 WHV-induced tumors (41%) contained rearrangements at N-*myc* loci due to viral genomic integration. Six of these seven inserts affected N-*myc*2, and most of these were at the 5′ end of the gene. In contrast, only two of seven GSHV-induced woodchuck HCCs expressed N-*myc* RNA, and only 1 of the 16 tumors (6%) contained a rearranged N-*myc* allele. The GSHV-associated HCCs all contained numerous viral insertions, so the low frequency of integration into N-*myc* loci by GSHV was not due to a general block to integration. Four of sixteen GSHV-induced tumors harbored amplified c-*myc* alleles, and five of seven GSHV tumors tested contained elevated c-*myc* RNA levels. By contrast, enhanced c-*myc* RNA levels were observed in only 2 of 13 WHV-induced HCC. We conclude that N-*myc* overexpression is a regular feature of WHV- but not GSHV-associated hepatocarcinogenesis in a common host. In contrast, c-*myc* transcriptional deregulation is rarely encountered in WHV-induced HCC but is frequent in GSHV-induced HCC.

Hepatocellular carcinoma (HCC) is one of the most common human cancers in the world, with the highest incidence occurring in Asia and sub-Saharan Africa. Persistent hepatitis B virus (HBV) infection is a significant risk factor for HCC in humans (2, 3). Worldwide, HBV is considered the likely etiologic agent for over 75% of HCC cases (3).

HBV is a member of the hepadnavirus family of small hepatotropic DNA viruses. Two genetically and antigenically related hepadnaviruses are found in wild rodents: woodchuck hepatitis virus (WHV) and ground squirrel hepatitis virus (GSHV). Like HBV, both viruses are associated with the development of HCC in their native hosts and thus represent experimental models of this important virus-associated malignancy. Interestingly, despite their close homology and identical replication strategies, the two viruses display reproducible differences in some aspects of hepatocarcinogenesis. In woodchucks chronically infected from birth with WHV, 100% will develop HCC within 17 to 36 months (15). In contrast, in captive ground squirrels with naturally acquired GSHV infection, HCC occurs less frequently and with a latency of 4 to 5 years or more (11).

Because GSHV is infectious for woodchucks (17), examination of the natural history of GSHV and WHV infections in this common host allows determination of whether these biological differences are of viral or host origin. Chronic GSHV infection in woodchucks produces mild to moderate portal hepatitis in woodchucks, similar to that observed in woodchucks chronically infected with WHV. However, in GSHV-infected woodchucks, HCC developed about 18 to 24 months later than in the WHV carriers (17). Thus, although both viruses are oncogenic in the woodchuck host, GSHV and WHV differ in oncogenic determinants that affect the course of HCC development in chronically infected animals.

Hepadnaviruses replicate their DNA genomes episomally; integration into the chromosome is not an obligate part of their life cycle. But chromosomal integration does occur at a low frequency and can affect the surrounding genes in a positive or negative way. Surveys of human liver tumors consistently show HBV genomic integrations that are clonally expanded in the tumor tissue, suggesting that integration is a relatively early event in carcinogenesis. The recent finding of N-*myc* activation by integration of WHV DNA in woodchuck HCC DNA (8) has given support to the hypothesis that integration of HBV into the host genome can contribute to oncogenesis.

There are two N-*myc* loci in the woodchuck genome: N-*myc*1, which is homologous to human and mouse N-*myc* genes, and N-*myc*2, which lacks introns and is apparently a functional retroposed copy of N-*myc*1. Fourel et al. (8) showed that 6 of 30 tumors examined contained WHV integrations at the N-*myc* loci, and all of these integrations interrupted the 3′ untranslated region of N-*myc*. Furthermore, N-*myc*2 was a more frequent target for integration (five of six tumors) than was N-*myc*1 (one out of six tumors).

Altered c-*myc* expression also has been observed in woodchuck and ground squirrel HCCs (9, 12, 24). The described c-*myc* alterations in woodchucks infected with WHV involved rearrangements of the c-*myc* locus. In one case, there was an apparent chromosomal translocation without any residual WHV genome within 5 kbp of the woodchuck c-*myc* gene (12); two other woodchuck tumors contained viral insertions near the woodchuck c-*myc* gene (9). In each case, the levels of c-*myc* RNA were 5- to 50-fold

* Corresponding author.

higher than in adjacent liver tissues. c-*myc* expression has also been found to be altered in HCCs from ground squirrels infected with GSHV. In this case, however, the c-*myc* gene was not found to be rearranged but instead was amplified by an unknown mechanism (24). N-*myc* involvement in ground squirrel HCCs has not been observed.

In this study, we examine genomic DNA from tumors arising in the WHV- and GSHV-infected woodchucks in order to determine whether these viruses use the same oncogenic pathway when replicating in a common host. Our results indicate that HCCs induced by infection with these closely related viruses display striking differences in expression of *myc* gene family members and in the mechanisms by which their expression is activated.

MATERIALS AND METHODS

Origin of the tumors. The majority of the tumors used in this study have been described previously (17). Newborn woodchucks were inoculated subcutaneously with WHV- or GSHV-containing serum. Of the original 39 WHV-induced tumors from 16 woodchucks, a total of 17 tumor samples from 7 animals were studied; 13 GSHV-induced tumors from 6 woodchucks were used. Three additional tumors arose in two GSHV-infected animals after the publication of our initial study and were included in the current analysis; these are designated G1697-T1, G1697-T2, and G2002-T1. Nontumorous liver samples were taken from each infected animal as sources of control DNA and RNA.

Nucleic acid analysis. Genomic DNA was prepared from each tumorous and nontumorous sample by crushing approximately 100 mg of tissue in a mortar under liquid nitrogen with 4 ml of DNA lysis buffer (0.25 M EDTA [pH 9.0], 1% sodium dodecyl sulfate, 500 μg of proteinase K per ml) and then incubating the samples at 55°C for 3 to 12 h. The samples were then extracted once with phenol-chloroform (pH 8.0) and precipitated with 1 volume of ethanol (room temperature). The DNA was spooled onto the end of a sealed Pasteur pipette, rinsed with 80% ethanol, and dissolved in 2 ml of a solution containing 5 mM EDTA (pH 7) and 250 μg of RNase A per ml. The DNA was incubated at 37°C for 30 min, 100 μl of a solution containing 0.4 M Tris (pH 8.3), 1 M sodium acetate, and 2 mg of proteinase K was added, and the samples were incubated at 50°C for 30 min. The samples were then extracted with phenol-chloroform and precipitated with 3 volumes of room temperature ethanol. The DNA was spooled onto the end of a Pasteur pipette, rinsed with 80% ethanol, briefly air dried, and dissolved in 0.25 to 0.5 ml of TE8 (10 mM Tris [pH 8.0], 1 mM EDTA).

For Southern blot analysis, approximately 10 μg of genomic DNA was digested with either *Hin*dIII or *Bgl*II for more than 8 h at 37°C and then subjected to ethanol precipitation. The restricted DNA samples were redissolved in H_2O and loading buffer (40% [wt/vol] sucrose, 0.25% bromophenol blue), heated at 65°C for 10 min, and fractionated by electrophoresis on a 1.0% agarose gel in Tris-borate buffer (2.5 mM EDTA, 45 mM borate, 133 mM Tris [pH 8.3]). The DNA was transferred onto a Hybond N membrane (Amersham) in 10× SSC (1.5 M NaCl, 0.15 M sodium citrate), cross-linked to the membrane by UV illumination, and hybridized to radiolabeled DNA probes at 65°C in Church hybridization buffer (6). The membranes were washed twice for 30 min at 65°C in Church wash buffer (6) and exposed to Kodak XAR film in the presence of an intensifying screen. When appropriate, the membranes were stripped by heating in Church wash buffer for 5 min at the high setting in a microwave oven. The extent of stripping was monitored by reexposure to Kodak XAR film.

Total RNA was prepared from the nontumorous and tumorous samples by the method of Chomczynski and Sacchi (5), using RNAzol B (Tel-Test, Inc.) according to the manufacturer's conditions. Yields of RNA were quantitated spectrophotometrically, and slot blot analysis was carried out by preparing 0.1, 1.0, and 10 μg of RNA for each sample in 2× SSC, heating the samples at 65°C, and applying them to Hybond N (Amersham) in a slot blot apparatus (Schleicher & Schuell) under vacuum. The membrane was washed three times with 0.5 ml of 6× SSC. The membrane was then cross-linked by UV irradiation and hybridized to the N-*myc* 3′ probe. The membrane was then stripped and reprobed with a c-*myc* probe.

Probe preparation. Purified DNA restriction fragments were radiolabeled by the random primer method (7). The 3.3-kbp cloned genomes of WHV2 (10) and GSHV (18) were used to make the virus-specific probes. The c-*myc* probe was contained on a 1.9-kbp *Hin*dIII restriction fragment from the murine cDNA clone pMcmyc 54 (21).

The N-*myc* 5′ and 3′ probes were generated by amplifying the genomic N-*myc*2 sequences from the nontumorous liver sample from woodchuck W1667. The primers used to generate the N-*myc* 5′ probe were from N-*myc* exon 1; sequences of the primers were 5′-**GGAATT**CTGGACGCGC TGAGTGGATGCGG-3′ (N-*myc*2 nucleotides −297 to −274 [8]; numbering is from the first ATG codon; boldface nucleotides are not present in the N-*myc* genome) and 5′-**GGAAT** TCCTGCAAATCATCCTCGGCATGGTG-3′ (complementary to N-*myc*2 nucleotides 21 to 47). A polymerase chain reaction (PCR) using these primers resulted in a 350-bp DNA fragment which contained *Eco*RI sites at each end. This DNA fragment was gel purified, digested with *Eco*RI, and cloned into plasmid pBS(−) (Stratagene). The primers used to create the N-*myc* 3′ probe were N-*myc*2-5′ (5′-**GGAAT** TCTGCCGTGGGCGCTGCGGTTGC-3′; N-*myc*2 nucleotides 637 to 659) and N-*myc*2-3′ (5′**GGAATT**CCACCAT CATTTGCTGTGATATCACTC-3′; complementary to N-*myc*2 nucleotides 2288 to 2316). PCR using these primers generated a 1.7-kbp DNA fragment which contained *Eco*RI sites at each end. This DNA fragment was gel purified, digested with *Eco*RI, and cloned into plasmid pBS(−).

A 9-kbp *Eco*RI genomic clone containing the N-*myc*1 gene was isolated from a size-selected *Eco*RI-lambda Dash II (Stratagene) library created from the nontumorous liver DNA from woodchuck W1667. A subclone containing a 1.4-kbp *Eco*RI DNA fragment was created by amplifying the first intron of N-*myc*1 by PCR using the N-*myc* exon 1 5′ and 3′ primers (described above). An N-*myc*1-specific probe was generated from this clone by digestion with *Sal*I and *Sph*I restriction endonucleases and isolation of the 1-kbp DNA fragment.

Cloning of the WHV/N-*myc* integration junctions. WHV/N-*myc*2 junctions were amplified from genomic DNA of WHV-associated tumors 1640-T1, 1654-T2, 1659-T1, and 1667-T1 by PCR, using one primer which hybridizes to N-*myc*2 and one primer which hybridizes to WHV. For the 5′ integration junction reactions, we used the following N-*myc*2 exon 1 3′ primer and primers from around the genome of WHV2 (10): EN1 (5′-**GGAATTC**CACACCACGCCACGTTGCC-3′, complementary to nucleotides 1286 to 1304, with an *Eco*RI site [boldface] added), EN2 (5′-**GGAATTC**GTGTTTGCTGA CGCAACCCC-3′; nucleotides 1309 to 1328, with an *Eco*RI site at the 5′ end), and DR1 (5′-**CGGGATCCCG**GGCACA GCTTGGAGGCTTGAAAAG-3′; complementary to nucle-

otides 1980 to 2003, with an engineered *Bam*HI site). The 5′ junction fragments for W1640-T1 (0.35 kbp) and W1659-T1 (0.6 kbp) were generated with primer EN2; the 0.8-kbp junction fragment of W1654-T2 was created with primer DR1. The 3′ junction fragment of W1667-T1 (0.8 kbp) was generated with primers EN1 and N-*myc* 3′2b (5′-**CGGG ATCCTGTGAGTATGTCCACTACCTC**-3′; N-*myc*2 nucleotides 1247 to 1269, with a *Bam*HI site at the 5′ end).

The amplified DNA fragments were digested with the appropriate restriction enzymes and cloned into Bluescript vectors (Stratagene). Sequence analysis (16) was performed on double-stranded DNA, using Sequenase enzyme (U.S. Biochemical) as recommended by the manufacturer.

RESULTS

N-*myc* RNA expression in WHV- and GSHV-associated woodchuck HCC. Activation of N-*myc* gene expression in WHV-induced HCC has been shown previously (8). To determine whether this is an obligate feature of hepatocarcinogenesis in woodchucks, we examined the level of N-*myc* expression in HCC arising from infection with either WHV or GSHV. Total RNA was prepared from available tumor samples, applied to membrane filters, and probed with radiolabeled N-*myc* DNA. Figure 1A shows the results obtained for WHV-induced tumors. In accord with an earlier report (8), we found that N-*myc* is not expressed in normal woodchuck liver (Fig. 1A, row 1); however, elevated levels of N-*myc* RNA were found in 10 of 13 WHV-associated tumors (in tumor W1667-T1, in which enhanced N-*myc* expression was not observed, extensive RNA degradation occurred). By contrast, N-*myc* up-regulation was seen in only two of the seven GSHV-associated specimens from which sufficient material was available for analysis (Fig. 1B). (This difference approaches but does not reach statistical significance [$P = 0.06$ in Fisher's exact test], an observation likely referable to the small sample size of GSHV-induced tumors examined.) These results indicate that N-*myc* activation is not obligatory for hepatocarcinogenesis in woodchucks and suggest that virus-specific differences in N-*myc* activation exist.

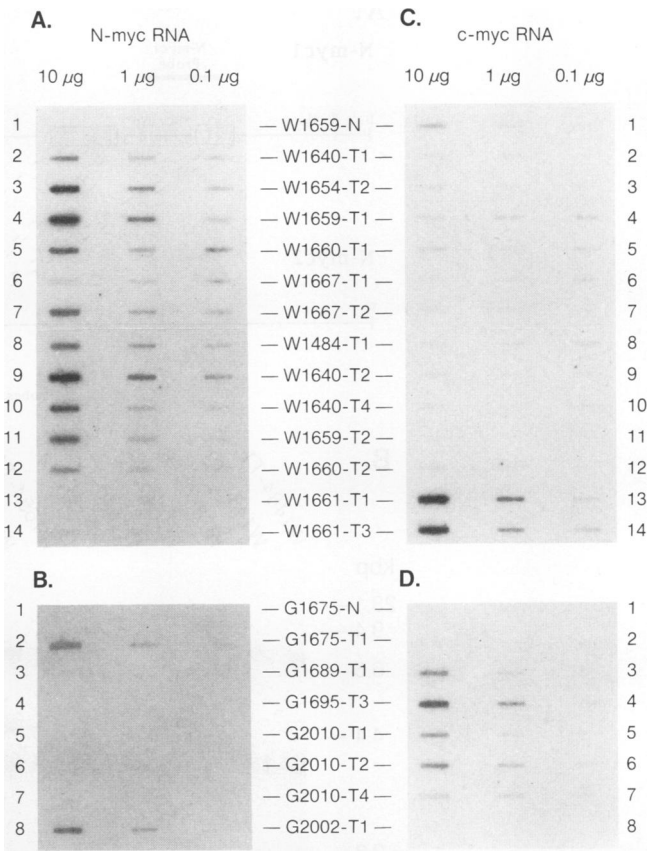

FIG. 1. Northern slot blot analysis of N-*myc* and c-*myc* RNA present in WHV- and GSHV-associated HCCs. (A and B) For each sample, 10, 1, and 0.1 μg of total RNA were applied to a nitrocellulose membrane and hybridized to a N-*myc* 3′ probe. (C and D) The membrane used in panels A and B was stripped and rehybridized with a murine cDNA c-*myc* probe. Tumor samples with a "W" prefix are derived from WHV-associated woodchuck HCCs; samples with a "G" prefix are derived from GSHV-associated woodchuck HCCs.

N-*myc* gene rearrangements in WHV-induced tumors. The restriction enzyme *Hin*dIII cuts outside of both N-*myc*1 and N-*myc*2 genes (Fig. 2A), liberating 7.4-kbp (N-*myc*1) and 3.5-kbp (N-*myc*2) DNA fragments. Southern blot analysis of *Hin*dIII-digested DNA from a total of 17 WHV-induced tumors probed for N-*myc* sequences showed that many of the tumors contained rearrangements of the woodchuck N-*myc* genes (15 of these tumors are shown in Fig. 2B). None of the rearrangements were present in matching nontumorous samples from each animal (data not shown). Tumors in Fig. 2B that contained new restriction fragments that hybridized to N-*myc* were W1640-T1, W1640-T4, W1654-T2, W1659-T1, W1660-T1, and W1667-T1. Several of the new N-*myc* restriction fragments also hybridized to a WHV-specific probe, suggesting that WHV insertion near N-*myc* had caused the rearrangement (data not shown). Two additional tumor samples not shown in Fig. 2, W1661-T1 and W1667-T2, were also examined; one of them (W1661-T2) was also found to contain submolar amounts of an N-*myc* rearrangement.

Samples containing novel N-*myc* *Hin*dIII restriction fragments were further analyzed to determine whether the WHV insertions were 5′ or 3′ with respect to the coding sequence of N-*myc*. Tumor DNA was digested with *Bgl*II, which separates the 5′ and 3′ portions of N-*myc*2 into 5.7- and 4.8-kbp restriction fragments, respectively (*Bgl*II cuts outside of N-*myc*1 to release a 9.2-kbp DNA fragment; Fig. 2A). Hybridization with the N-*myc* 5′ probe revealed several novel restriction fragments in the Southern blot analysis (Fig. 3A). Tumors W1640-T1, W1654-T2, and W1659-T1 (Fig. 3A, lanes 2, 4, and 5) all showed evidence for rearrangement at the 5′ end of N-*myc*. The unique bands from these three tumors did not hybridize with the N-*myc* 3′ probe (Fig. 3B), which suggested that the affected N-*myc* gene was the N-*myc*2 locus. Sample W1667-T1 contained an additional DNA fragment which only hybridized to the 3′ probe (Fig. 3B, lane 8). The large additional N-*myc* DNA fragment in sample W1660-T1 (Fig. 3, lanes 7) hybridized to both probes, which suggested that the rearrangement was in the N-*myc*1 locus. These observations were further substantiated by hybridization to an N-*myc*1-specific probe; the only new fragment which hybridized to this probe was the one from sample W1660-T1 (data not shown). The minor rearrangements in W1640-T4 and W1667-T2 (not shown) could not be assigned to the 5′ or 3′ end of N-*myc* in this analysis. Taken together, our results showed that N-*myc* was a frequent target for rearrangement (7 of 17 tumors; 41%) and that the N-*myc*2 locus was preferred over N-*myc*1 (6 of 7; 86%).

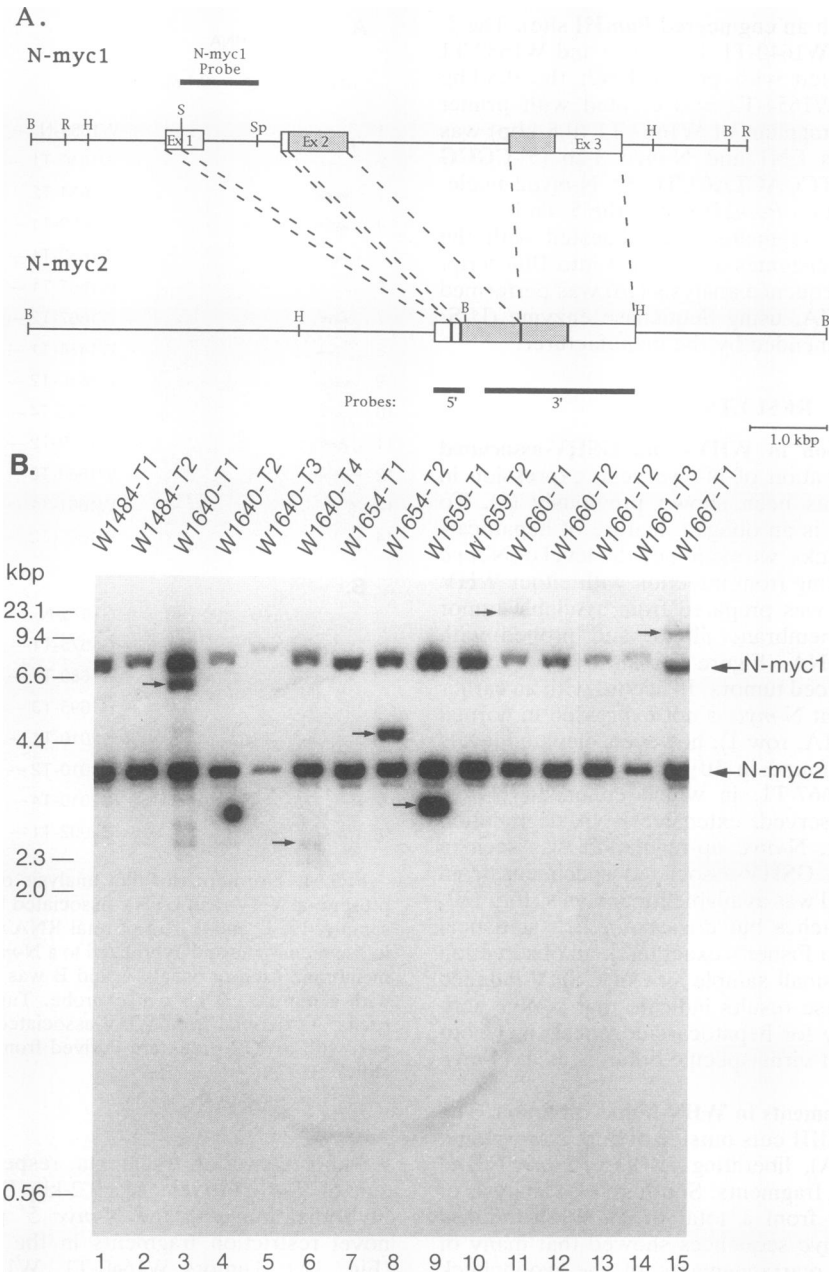

FIG. 2. N-*myc* rearrangements in WHV-induced woodchuck HCC. (A) Restriction maps of N-*myc*1 and N-*myc*2 (adapted from reference 8). Boxes denote exons; open boxes denote noncoding sequence, and the stippled boxes represent coding sequence. Regions that are homologous to the known exons of the human and murine N-*myc* genes are indicated by Ex 1, Ex 2, and Ex 3. N-*myc*2 regions of homology with N-*myc*1 are aligned with dotted lines. The N-*myc*1-specific probe, indicated above the N-*myc*1 gene, consists of a 1.0-kbp *Sal*I-*Sph*I fragment. The N-*myc* 5′ and 3′ probes are diagrammed under the N-*myc*2 gene. B, *Bam*HI; H, *Hin*dIII; R, *Eco*RI; S, *Sal*I; Sp, *Sph*I. (B) Southern blot analysis of *Hin*dIII-digested DNA from WHV-induced HCCs, hybridized with the N-*myc* 3′ probe. Arrows indicate novel restriction fragments that contain N-*myc* DNA.

Most of the rearrangements were found to be at the 5′ end of N-*myc*2, in contrast to an earlier study (8) in which six of six WHV-associated N-*myc*2 rearrangements were at the 3′ end. More recent studies also have demonstrated rearrangements at the 5′ end of N-*myc*2 (25).

The results from the Southern blot analysis suggested that the N-*myc* rearrangements were most likely due to WHV integration. To show this directly, several of the WHV/N-*myc* junctions were cloned by PCR, using either a 5′ or 3′ N-*myc*2 primer paired with primers from around the WHV genome. The junctions for three 5′ insertions and one 3′ insertion were obtained in this way; the results of this analysis are shown schematically in Fig. 4. Primers from the WHV enhancer region, EN1 and EN2, were used to clone three of the four junctions. The other primer used in this analysis, DR1, comes from a region important in the replication of the viral DNA (19). This region has been reported to be often near chromosomal integration junctions of HBV

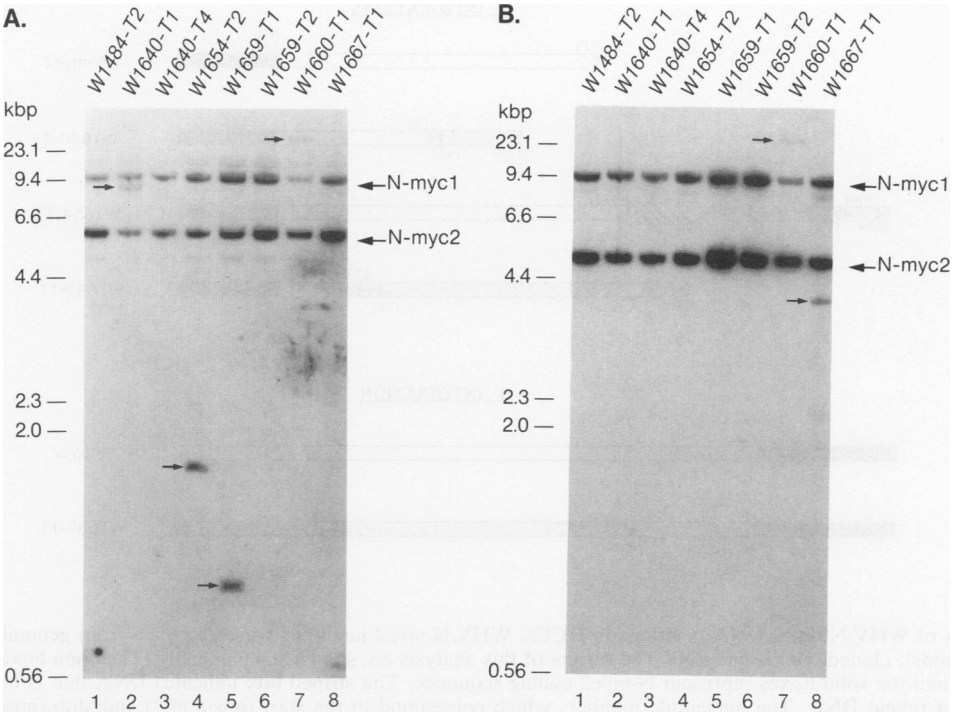

FIG. 3. Southern blot analysis of the 5′ and 3′ regions of N-*myc*2 in the WHV-induced HCCs. Selected tumor DNA samples were digested with *Bgl*II and analyzed by hybridization to N-*myc* 5′ (A) and 3′ (B) probes. Arrows indicate novel restriction fragments that contain N-*myc* DNA.

in human HCC (14). The 5′ rearrangements occurred 55 (W1659-T1), 196 (W1640-T1), and 462 (W1654-T2) bp upstream of the start codon of N-*myc*2 (Fig. 4). The WHV genomes in W1654-T2 and W1659-T1 were found to be rearranged, an occurrence often observed for integrated sequences of HBV (22). Also, in tumor W1654-T2, a sequence of approximately 100 nucleotides in genomic woodchuck DNA found between the WHV insertion and published N-*myc*2 sequences was found to be homologous to a repetitive DNA sequence located in the nontranscribed spacers of rat rRNA genes (13, 27). The WHV insertion into the 3′ region of N-*myc*2 in W1667-T1 was found to be 159 bp downstream of the N-*myc*2 stop codon (Fig. 4).

N-*myc* loci in GSHV-associated woodchuck tumors. Genomic tumor DNA from GSHV-infected woodchucks was examined for rearrangements in N-*myc* loci. The results of Southern blot analysis of *Hin*dIII-digested DNA, probed with radiolabeled N-*myc* DNA, are shown in Fig. 5. Only 1 of 16 samples (~6%) showed an N-*myc* rearrangement, a frequency strikingly lower than that found in the WHV-associated tumors (~41%); this difference is statistically significant ($P = 0.039$ in Fisher's exact test). The novel N-*myc* restriction fragment of G1675-T1 migrated with an apparent mobility of about 1 kbp.

The GSHV-associated N-*myc* rearrangement was mapped by digesting the tumor DNA with *Bgl*II and subjecting it to Southern blotting (Fig. 6). Hybridization with the N-*myc* 5′ probe revealed only the genomic copies of N-*myc*1 (9.2 kbp) and N-*myc*2 (5.7 kbp) (Fig. 6A). However, the N-*myc* 3′ probe showed two novel bands, approximately 0.8 and 2.2 kbp, in the G1675-T1 tumor DNA. Hybridization to the 3′ probe indicates that N-*myc*2 was rearranged. The 1-kbp *Hin*dIII fragment (Fig. 5, lane 1) did not hybridize to an N-*myc*1-specific probe (data not shown), further substantiating the involvement of the N-*myc*2 locus. Attempts to clone the GSHV/N-*myc*2 junction by PCR using a primer from the 3′ end of N-*myc*2 paired with each of several primers from around the GSHV genome were unsuccessful.

GSHV integrations have been reported to occur at a relatively low frequency in GSHV-associated ground squirrel HCCs (24). To address the possibility that the N-*myc* loci were infrequent targets for GSHV integration because GSHV itself had a low frequency of integration into the woodchuck genome, a GSHV-specific DNA probe was used in Southern blot analysis of *Hin*dIII-digested tumor DNA (Fig. 7). The results of this analysis showed that all of the GSHV-associated HCCs examined contained multiple integrations of GSHV into the tumor DNA. The novel 1-kbp N-*myc*-hybridizing DNA fragment from sample G1675-T1 (Fig. 5) did not hybridize to the GSHV probe (Fig. 7). Several possibilities could explain this observation: (i) the rearrangement in this sample may not be due to GSHV integration; (ii) a subsequent rearrangement that separated the GSHV and the N-*myc* sequences may have occurred; or (iii) insufficient GSHV sequences remain in that restriction fragment to allow hybridization to the GSHV probe.

It is interesting to note that tumor G1675-T1 was the largest (4 cm) and earliest GSHV-associated tumor to arise (31 months postinoculation) in our earlier study (17). In addition, this tumor locus was one of the two GSHV-associated HCCs displaying up-regulation of N-*myc* RNA.

c-*myc* gene amplification in the WHV- and GSHV-associated HCCs. Because altered c-*myc* expression has been observed in woodchuck and ground squirrel HCCs (9, 12, 24), the c-*myc* locus was examined in our set of WHV- and GSHV-associated woodchuck HCCs. Southern blot analysis of the

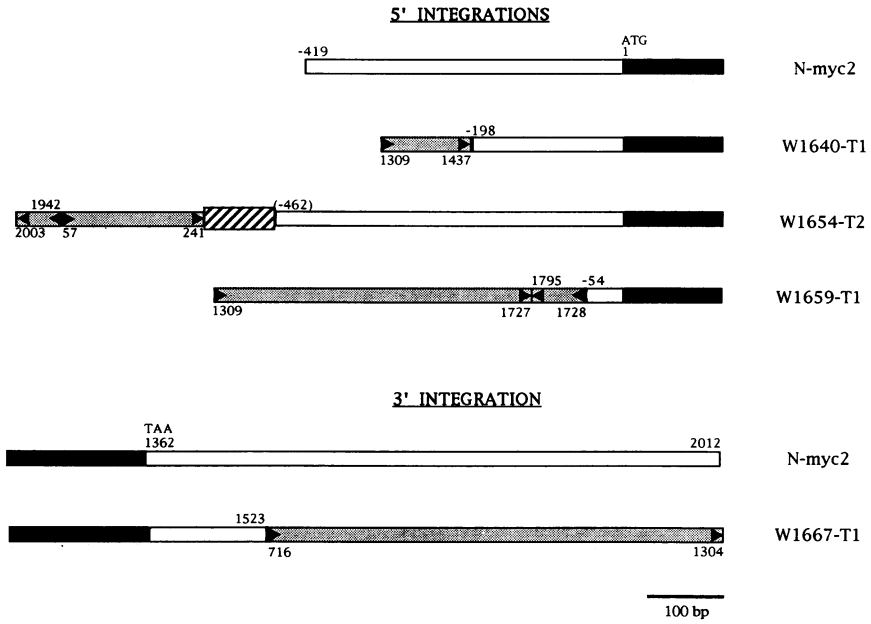

FIG. 4. Analysis of WHV/N-*myc*2 DNA junctions in HCCs. WHV/N-*myc*2 junctions were amplified from genomic DNA by PCR (see Materials and Methods), cloned, and sequenced. The results of this analysis are shown schematically. The open boxes indicate noncoding N-*myc*2 sequence, and the solid boxes represent N-*myc*2 coding sequence. The striped box indicates DNA that is homologous to rat and mouse rRNA spacer repeat DNA. The nucleotide numbers which correspond to the start (position 1) and stop (position 1362) codons in N-*myc*2 (8) are indicated in the N-*myc*2 diagrams; the nucleotide position of the N-*myc*2 junction is indicated for each tumor. The nucleotide sequences delineating the WHV components are shown in stipple; their nucleotide position (position 10) in the viral genome is shown above or below each line. The arrowheads indicate the direction of the coding sequence of WHV.

WHV tumor DNA, using a c-*myc* probe, showed that 2 of the 17 (12%) tumors displayed amplification of the 8-kbp *Hin*dIII restriction fragment containing the woodchuck c-*myc* locus (Fig. 8, lanes 13 and 15). (The digestion of the W1661-T1 DNA [lane 13] with *Hin*dIII was incomplete. To verify that amplification occurred and to quantify its extent, Southern blot analysis was repeated by using DNA from nontumorous liver, W1661-T1, and W1661-T3, each completely digested with *Bgl*II; blots were probed with c-*myc* and N-*myc* probes, the latter as an internal standard [data

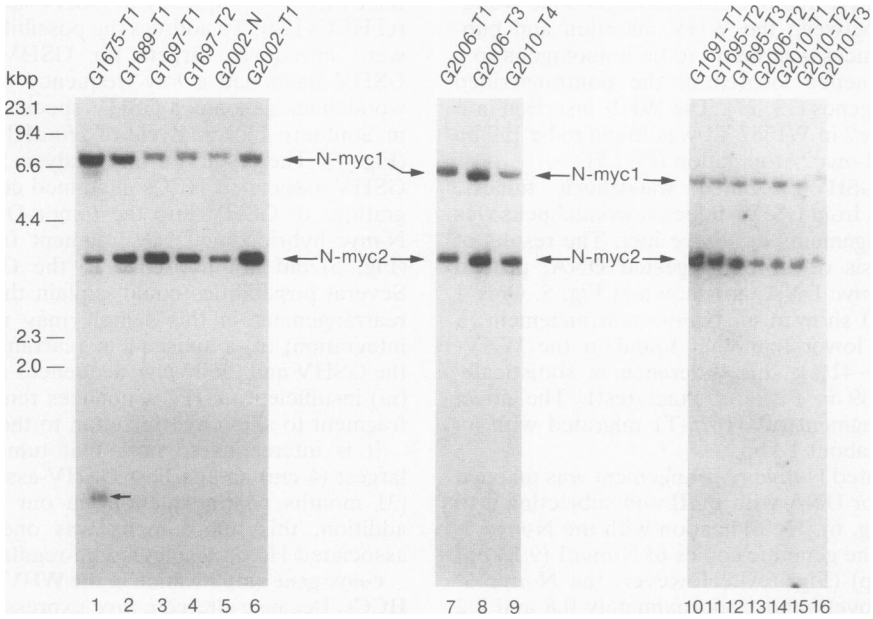

FIG. 5. N-*myc* rearrangement in GSHV-induced woodchuck HCC. Shown is Southern blot analysis of the *Hin*dIII-digested DNA from GSHV-induced HCCs, hybridized with the N-*myc* 3′ probe. The arrow indicates the novel restriction fragment that contains N-*myc* DNA. DNA from a nontumorous liver sample is shown in lane 5.

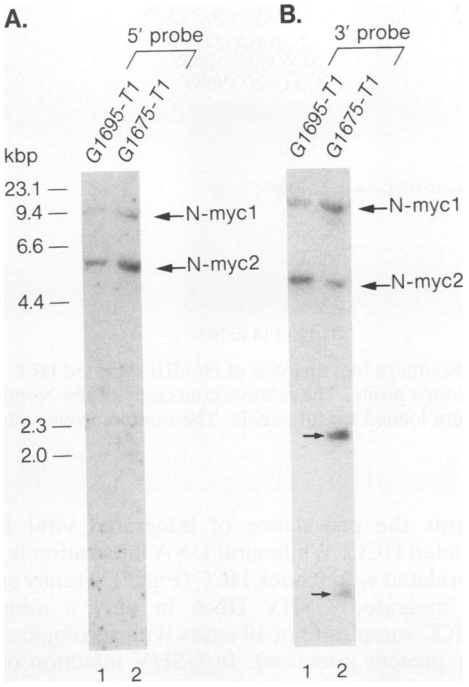

FIG. 6. Southern blot analysis of the 5′ and 3′ regions of N-*myc*2 in two GSHV-induced HCCs. Selected tumor DNA samples were digested with *Bgl*II and analyzed by hybridization to N-*myc* 5′ (A) and 3′ (B) probes. The blot shown in panel B was stripped and reprobed with the N-*myc* 5′ probe (A). Arrows indicate novel restriction fragments that contain N-*myc* DNA.

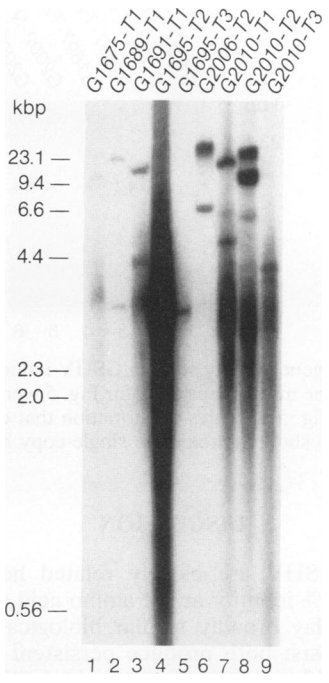

FIG. 7. GSHV genomic integrations into woodchuck HCC DNA. Shown is Southern blot analysis of *Hin*dIII-digested DNA from GHSV-induced HCCs. The DNA samples used in lanes 1 and 2 correspond to the DNA samples used in Fig. 5, lanes 1 and 2, respectively. Lanes 3 to 9 are identical to lanes 10 to 16 of Fig. 5, for which the membrane has been stripped and reprobed with the GSHV probe.

not shown]. This analysis confirmed that there was no rearrangement at the c-*myc* locus, and densitometric analysis showed that c-*myc* DNA in W1661-T1 was amplified approximately 14-fold, while the c-*myc* locus from W1661-T3 [lane 15] was amplified ca. 4-fold.) This form of genetic alteration of c-*myc* differs from those previously observed in WHV-associated HCC, namely, integration of WHV DNA into the c-*myc* locus (9). Amplification of the c-*myc* locus has been observed, however, in GSHV-associated ground squirrel HCCs (24) as well as in other hepatocellular carcinomas (4, 23).

c-*myc* expression in the WHV-associated HCCs was analyzed by stripping the RNA slot blot previously used to examine N-*myc* expression and then hybridizing the blot with the radiolabeled c-*myc* DNA probe (Fig. 1C). The only tumor samples that overexpressed c-*myc* RNA were the two WHV HCCs that contained amplified c-*myc* DNA (Fig. 1C, rows 13 and 14; Fig. 8, lanes 13 and 15).

The genetic disposition of the c-*myc* locus in the GSHV-associated HCCs was examined by reprobing the *Hin*dIII-digested DNA Southern blots with the c-*myc* probe (Fig. 9). The c-*myc* alterations were again found to be gene amplifications rather than viral insertions. DNA from nontumorous samples was included to indicate single-copy hybridization. Four of the 16 (25%; Fig. 9, lanes 2, 3, 13, and 16) GSHV-associated tumors contained amplified c-*myc* DNA, a frequency comparable to that previously reported in HCCs from ground squirrels naturally infected with GSHV (6 of 14; 43% [24]).

The pattern of c-*myc* expression in the GSHV-associated tumors is shown in Fig. 1D. Five of the seven GSHV tumors analyzed (71%) express c-*myc* RNA (Fig. 1D, rows 3 to 7). The only two GHSV tumors that did not express c-*myc* were the tumors that expressed N-*myc* (rows 2 and 8). Each tumor with amplified c-*myc* DNA showed c-*myc* expression (rows 3, 4, and 6). In addition, two tumor samples that lacked c-*myc* amplification also expressed c-*myc* RNA (rows 5 and 7). Taken together, the RNA analysis of GHSV- and WHV-associated tumors showed a reciprocal relationship between expression of N-*myc* and c-*myc*. N-*myc* expression occurred more frequently in WHV-associated HCCs, whereas c-*myc* expression was observed in the majority of GSHV-associated HCCs. Coexpression of both N-*myc* and c-*myc* was never observed in these HCC DNAs.

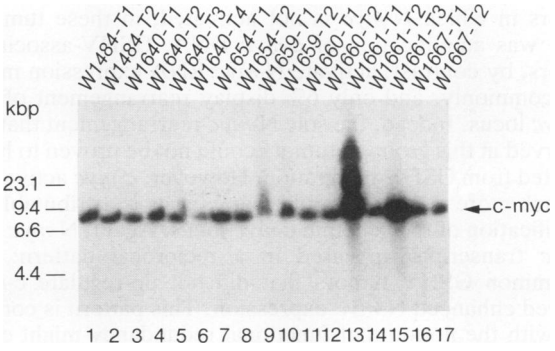

FIG. 8. c-*myc* gene amplification in WHV-induced woodchuck HCC. Shown is Southern blot analysis of *Hin*dIII-digested HCC DNA hybridized to the murine cDNA c-*myc* probe. The DNA in lane 13 is incompletely digested by the restriction enzyme (see text).

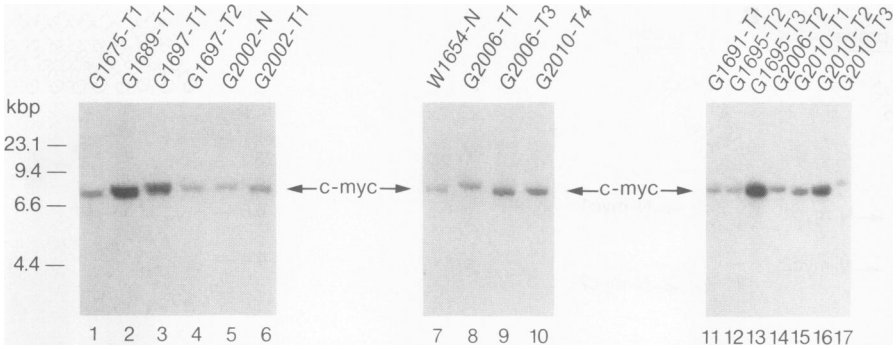

FIG. 9. c-*myc* gene amplification in GSHV-induced woodchuck HCC. Shown is Southern blot analysis of *Hin*dIII-digested HCC DNA; in this experiment, the membranes used for Fig. 5 were stripped and reprobed with a c-*myc* probe. The relative constancy of the N-*myc*1 signal in each panel of Fig. 5 provides confirmation that comparable amounts of DNA were loaded for all panels. The nontumorous sample (lane 7) was included to show approximate single-copy hybridization.

DISCUSSION

WHV and GSHV are closely related hepadnaviruses, sharing 71 to 92% identity at the amino acid sequence level (18). They display broadly similar biological behaviors in their natural hosts: both produce persistent hepatic infections with variable grades of chronic hepatitis, and each is associated with the development of hepatic neoplasms in its natural host. However, tumors arise with a remarkably different time course in the two infections (11, 15), and this difference is reproduced when the two viruses are studied in parallel in a common host (woodchuck) (17). Thus, viral determinants clearly contribute to these biological differences, but little is known about these viral factors and how they might operate in hepatocarcinogenesis.

In this work, we have examined the molecular phenotype of the woodchuck HCCs arising in the context of the two viral infections. Our results indicate the presence of both common themes and major variations. In both sets of tumors, activation of expression of members of the *myc* family of nuclear proto-oncogenes occurs, suggesting an important role for these gene products in oncogenesis. However, the pattern of which family members are activated and the mechanisms by which activation occurs clearly differ between the two infections.

Virtually all WHV-induced tumors display enhanced N-*myc* expression and, in nearly half of these cases, up-regulation is presumably due to insertional activation of the locus by regulatory elements in adjacent WHV DNA (8, 25). Activation of c-*myc* expression is rare, being limited to those tumors in which N-*myc* is not activated; in these tumors, there was amplification of c-*myc* DNA. GSHV-associated tumors, by contrast, activate N-*myc* RNA expression much less commonly, and only 6% display rearrangement of the N-*myc* locus. Indeed, the sole N-*myc* rearrangement that we observed in this group of tumors could not be proven to have resulted from GSHV integration. However, c-*myc* activation is much more common and in many cases is attributable to amplification of the genomic c-*myc* locus. Again, N-*myc* and c-*myc* transcripts appeared in a reciprocal pattern: the uncommon GSHV tumors that did not up-regulate c-*myc* showed enhanced N-*myc* expression. This pattern is consistent with the notion that functional redundancy might exist among *myc* gene family members.

In general, the oncogenic behavior of GSHV in the woodchuck host parallels its behavior in its natural host, the Beechey ground squirrel. The only discordance noted thus far concerns the prevalence of integrated viral DNA in GSHV-related HCC. While viral DNA integration is the rule in GSHV-related woodchuck HCC (Fig. 7), Transy et al. (24) detected integrated GSHV DNA in only a minority of squirrel HCC samples (3 of 10 cases with serologic evidence of past or present infection). In GSHV infection of woodchuck hosts, HCC arises in the context of active, ongoing infection with persistent viremia, while squirrel HCCs are often observed in elderly animals whose serologic markers indicate a resolved prior infection (i.e., no ongoing intrahepatic replication or viremia). We do not presently understand the basis for this difference. We note, however, that HCC is sometimes observed in squirrels with no serologic evidence of past or present GSHV infection (4 of 14 cases in the series of Transy et al. [24]). This finding raises the possibility that hepatic malignancies unrelated to viral infection (e.g., spontaneous tumors or carcinomas arising from unrecognized dietary or environmental factors) may be more frequent in squirrels than in woodchucks. If true, this could contribute to a higher higher background of virus-negative tumors among infected animals.

Our results allow us to exclude some models for the differential activation of *myc* gene family members by the two viruses. For instance, it is unlikely that the absence of N-*myc* insertions in squirrel HCCs is due to an inability of the squirrel N-*myc* loci to transform hepatocytes, since even fully transformation-competent woodchuck N-*myc* loci are not activated by GSHV infection in woodchuck cells. Likewise, we believe that a general block to GSHV integration cannot account for our observations. In principle, the dearth of viral insertions near N-*myc* in GSHV-related HCCs could reflect either an inability of the viral DNA to be inserted into this chromosomal region or an inability of GSHV *cis*-acting signals to activate expression of this locus.

In many woodchuck tumors, N-*myc* expression is up-regulated in the absence of a nearby viral integration. Little is known about how this occurs. In fact, the mechanism by which N-*myc* expression is extinguished in normal rodent liver cells is controversial; one group emphasizes repression of primary transcription (20), while another favors posttranscriptional control (1). It is hard to envision how insertion of viral DNA 5′ to the transcription unit could enhance expression of N-*myc* if regulation were controlled entirely by posttranscriptional mechanisms. But however this control is achieved, our results indicate that its disruption in viral carcinogenesis displays virus specificity. Thus, N-*myc* acti-

vation is not simply an invariable secondary consequence of the transformed phenotype. We doubt that activation of chromosomal N-*myc* loci is the direct result of transactivation by WHV X protein, since N-*myc* RNA is not expressed in the surrounding, nonneoplastic liver, which is densely infected and displays prominent evidence of viral gene expression (26).

The differences in the oncogenic behaviors of GSHV and WHV in a common host indicate that hepadnaviruses may use multiple pathways in hepatocarcinogenesis. Insertional mutagenesis of N-*myc* loci in WHV infection provides the clearest example to date of one step in such a pathway. The definition of the other steps in this pathway and the identification of other pathways remain outstanding challenges in this area of research.

ACKNOWLEDGMENTS

We thank T. L. Wright for help with statistical analysis of the data.

This work was supported by the Howard Hughes Medical Institute.

REFERENCES

1. **Babiss, L. E., and J. M. Friedman.** 1990. Regulation of N-*myc* gene expression: use of an adenovirus vector to demonstrate posttranscriptional control. Mol. Cell. Biol. **10:**6700–6708.
2. **Beasley, R. P.** 1988. Hepatitis B virus: the major etiology of hepatocellular carcinoma. Cancer **61:**1942–1956.
3. **Beasley, R. P., C.-C. Lin, L.-Y. Hwang, and C.-S. Chien.** 1981. Hepatocellular carcinoma and hepatitis B virus. Lancet **ii:**1129–1133.
4. **Chandar, N., B. Lombardi, and J. Locker.** 1989. c-*myc* gene amplification during hepatocarcinogenesis by a choline-devoid diet. Proc. Natl. Acad. Sci. USA **86:**2703–2707.
5. **Chomczynski, P., and N. Sacchi.** 1987. Single-step method of RNA isolation by acid guanidinium thiocyanate-phenol-chloroform extraction. Anal. Biochem. **162:**156–159.
6. **Church, G. M., and W. Gilbert.** 1984. Genomic sequencing. Proc. Natl. Acad. Sci. USA **81:**1991–1995.
7. **Feinberg, A. P., and B. Vogelstein.** 1983. A technique for radiolabeling DNA restriction endonuclease fragments to high specific activity. Anal. Biochem. **132:**6–13.
8. **Fourel, G., C. Trepo, L. Bougueleret, B. Henglein, A. Ponzetto, P. Tiollais, and M.-A. Buendia.** 1990. Frequent activation of N-*myc* genes by hepadnavirus insertion in woodchuck liver tumours. Nature (London) **347:**294–298.
9. **Hsu, T., T. Moroy, J. Etiemble, A. Louise, C. Trepo, P. Tiollais, and M.-A. Buendia.** 1988. Activation of c-*myc* by woodchuck hepatitis virus insertion in hepatocellular carcinoma. Cell **55:**627–635.
10. **Kodama, K., N. Ogasawara, H. Yoshikawa, and S. Murakami.** 1985. Nucleotide sequence of a cloned woodchuck hepatitis virus genome: evolutional relationship between hepadnaviruses. J. Virol. **56:**978–986.
11. **Marion, P. L., M. J. Van Davelaar, S. S. Knight, F. H. Salazar, G. Garcia, H. Popper, and W. S. Robinson.** 1986. Hepatocellular carcinoma in ground squirrels persistently infected with ground squirrel hepatitis virus. Proc. Natl. Acad. Sci. USA **83:**4543–4546.
12. **Moroy, T., A. Marchio, J. Etiemble, C. Trepo, P. Tiollais, and M.-A. Buendia.** 1986. Rearrangement and enhanced expression of c-*myc* in hepatocellular carcinoma of hepatitis virus infected woodchucks. Nature (London) **324:**276–279.
13. **Mroczka, D. L., B. Cassidy, H. Busch, and L. I. Rothblum.** 1984. Characterization of rat ribosomal DNA. J. Mol. Biol. **174:**141–162.
14. **Nagaya, T., T. Nakamura, T. Tokino, T. Tsurimoto, M. Imai, T. Mayumi, K. Kamino, K. Yamamura, and K. Matsubara.** 1987. The mode of hepatitis B virus DNA integration in chromosomes of human hepatocellular carcinoma. Genes Dev. **1:**773–782.
15. **Popper, H., L. Roth, R. H. Purcell, B. C. Tennant, and J. L. Gerin.** 1987. Hepatocarcinogenicity of the woodchuck hepatitis virus. Proc. Natl. Acad. Sci. USA **84:**866–870.
16. **Sanger, F., S. Nicklen, and A. R. Coulson.** 1977. DNA sequencing with chain-terminating inhibitors. Proc. Natl. Acad. Sci. USA **74:**5463–5467.
17. **Seeger, C., B. Baldwin, W. E. Hornbuckle, A. E. Yeager, B. C. Tennant, P. Cote, L. Ferrell, D. Ganem, and H. E. Varmus.** 1991. Woodchuck hepatitis virus is a more efficient oncogenic agent than ground squirrel hepatitis virus in a common host. J. Virol. **65:**1673–1679.
18. **Seeger, C., D. Ganem, and H. E. Varmus.** 1984. Nucleotide sequence of an infectious molecularly cloned genome of ground squirrel hepatitis virus. J. Virol. **51:**367–375.
19. **Seeger, C., and J. Maragos.** 1989. Molecular analysis of the function of direct repeats and a polypurine tract for plus-strand DNA priming in woodchuck hepatitis virus. J. Virol. **63:**1907–1915.
20. **Smith, R. K., K. Zimmerman, G. D. Yancopoulos, A. Ma, and F. W. Alt.** 1992. Transcriptional down-regulation of N-*myc* expression during B-cell development. Mol. Cell. Biol. **12:**1578–1584.
21. **Stanton, L. W., P. D. Farhlander, P. M. Tesser, and K. B. Marcu.** 1984. Nucleotide sequence comparison of normal and translocated murine c-myc genes. Nature (London) **310:**423–425.
22. **Takada, S., Y. Gotoh, S. Hayashi, M. Yoshida, and K. Koike.** 1990. Structural rearrangement of integrated hepatitis B virus DNA as well as cellular flanking DNA is present in chronically infected hepatic tissues. J. Virol. **64:**822–828.
23. **Tashiro, F., S. Morimura, K. Hayashi, R. Makino, H. Kawamura, N. Horikoshi, K. Nemoto, K. Ohtsubo, T. Sugimura, and Y. Ueno.** 1986. Expression of the c-Ha-ras and c-*myc* genes in aflatoxin B1-induced hepatocellular carcinomas. Biochem. Biophys. Res. Commun. **138:**858–864.
24. **Transy, C., G. Fourel, W. S. Robinson, P. Tiollais, P. L. Marion, and M.-A. Buendia.** 1992. Frequent amplification of c-*myc* in ground squirrel liver tumors associated with past or ongoing infection with a hepadnavirus. Proc. Natl. Acad. Sci. USA **89:**3874–3878.
25. **Wei, Y., G. Fourel, A. Ponzetto, M. Silvestro, P. Tiollais, and M.-A. Buendia.** 1992. Hepadnavirus integration: mechanisms of activation in the N-*myc*2 retrotransposon in woodchuck liver tumors. J. Virol. **66:**5265–5276.
26. **Yang, D., E. Alt, and C. Rogler.** Personal communication.
27. **Yavachev, L. P., O. I. Georgiev, E. A. Braga, T. A. Avdonina, A. E. Bogomolova, V. B. Zhurkin, V. V. Nosikov, and A. A. Hadjiolov.** 1986. Nucleotide sequence analysis of the spacer regions flanking the rat rRNA transcription unit and identification of repetitive elements. Nucleic Acids Res. **14:**2799–2810.